

Vibha Vansola, Surjit Mukherjee, Haladhara Naik*, Saraswatula Venkata Suryanarayana, Reetuparna Ghosh, Sylvia Badwar, Bioletty Mary Lawriniang and Yerraguntla Santhi Sheela

Determination of $^{55}\text{Mn}(n,\gamma)^{56}\text{Mn}$ reaction cross-section at the neutron energies of 1.12, 2.12, 3.12 and 4.12 MeV

DOI 10.1515/ract-2016-2610

Received April 4, 2016; accepted June 2, 2016; published online

July 22, 2016

Abstract: The $^{55}\text{Mn}(n,\gamma)^{56}\text{Mn}$ reaction cross-sections at the neutron energies of 1.12, 2.12, 3.12 and 4.12 MeV were determined by using activation and off-line γ -ray spectrometric technique. The neutron energies of 1.12 and 2.12 MeV were generated from the $^7\text{Li}(p,n)$ reaction by using the proton energies of 3 and 4 MeV from the folded tandem ion beam accelerator (FOTIA) at BARC. For the neutron energies of 3.12 and 4.12 MeV, the proton energies used were 5 and 6 MeV from the Pelletron facility at TIFR, Mumbai. The $^{115}\text{In}(n,\gamma)^{116\text{m}}\text{In}$ reaction cross-section was used as the neutron flux monitor. The $^{55}\text{Mn}(n,\gamma)^{56}\text{Mn}$ reaction cross-section at the neutron energies of 4.12 MeV are reported for the first time, whereas at 1.12, 2.12 and 3.12 MeV, they are in between the literature data. The $^{55}\text{Mn}(n,\gamma)^{56}\text{Mn}$ reaction cross-section was also calculated theoretically by using the computer code TALYS 1.6 and EMPIRE 3.2.2. The experimental data of present work are found to be in between the theoretical values of TALYS and EMPIRE.

Keywords: $^{55}\text{Mn}(n,\gamma)^{56}\text{Mn}$ reaction cross-section, off-line γ -ray spectrometric technique, $^{115}\text{In}(n,\gamma)^{116\text{m}}\text{In}$ reaction monitor, TALYS and EMPIRE calculation.

*Corresponding author: Haladhara Naik, Radiochemistry Division, Bhabha Atomic Research Center, Trombay, Mumbai-400085, India, E-mail: naikhbarc@yahoo.com

Vibha Vansola and Surjit Mukherjee: Department of Physics, Faculty of Science, M. S. University of Baroda, Vadodara-390002, India

Saraswatula Venkata Suryanarayana: Nuclear Physics Division, Bhabha Atomic Research Centre, Mumbai-400085, India

Reetuparna Ghosh, Sylvia Badwar and Bioletty Mary Lawriniang: Department of Physics, North Eastern Hill University, Shillong, Meghalaya-793022, India

Yerraguntla Santhi Sheela: Department of Statistics, Manipal University, Manipal-576104, India

1 Introduction

Manganese is one of the most abundant elements in the earth's crust. It is a gray white metal with a melting point of 1245°C and density of 7.43 g/cm³. As it has properties like sulfide former and deoxidizer and has hardenability, it is used in making steel and used as shielding material and structural material in reactors. Manganese has only one stable isotope ^{55}Mn with 100% abundance. In a reactor, neutrons interact with the ^{55}Mn , present in the shielding material and produce ^{56}Mn having the half life of 2.5789 h, which decay with the emission of 846.8 keV γ ray. Thus it affects the neutron economy in conventional reactor, advanced heavy water reactor (AHWR) [1], fast reactor [2–5], and accelerated driven sub-critical system (ADSs) [6–11]. The neutron spectrum in any conventional and fast reactors varies from thermal to 15–20 MeV. Thus it is necessary to have knowledge about the $^{55}\text{Mn}(n,\gamma)^{56}\text{Mn}$ reaction cross-section at different neutron energies, which are necessary for the design of the above mentioned reactors. Besides this, the knowledge of $^{55}\text{Mn}(n,\gamma)^{56}\text{Mn}$ reaction cross section is also important for better understanding of reaction mechanism.

It can be seen from the IAEA-EXFOR compilation [12] based on literature [13–30] data that, sufficient data on the $^{55}\text{Mn}(n,\gamma)^{56}\text{Mn}$ reaction cross-sections are available within the neutron energy of 4 MeV and around 13.4–15 MeV. Only one set of data within the neutron energies of 0.97–19.4 MeV, have been reported by Menlove et al. [19]. However, within the neutron energy of 4 MeV, there is lot of difference in the data based on the experimental work of various authors [16–30]. In view of this, the $^{55}\text{Mn}(n,\gamma)^{56}\text{Mn}$ reaction cross-sections at the neutron energies of 1.12, 2.12, 3.12 and 4.12 MeV have been determined by using an activation and off-line γ -ray spectrometric technique. The $^{55}\text{Mn}(n,\gamma)^{56}\text{Mn}$ reaction cross-section as a function of neutron energy was also calculated using the computer code TALYS 1.6 [31] and EMPIRE 3.2.2 [32]. The present data were compared with the literature data

[15–30] and the theoretical values based on TALYS 1.6 [31] and EMPIRE 3.2.2 [32].

2 Experimental details

The experiments with the neutron energies of 3.12 and 4.12 MeV were carried out by using the 14 UD BARC-TIFR (Bhabha Atomic Research Centre–Tata Institute of Fundamental Research) Pelletron facility at Mumbai, India [33]. The neutron beams were obtained from the $^7\text{Li}(p,n)^7\text{Be}$ reaction by using the proton beam of 5 and 6 MeV in the main line, 6 m above the analyzing magnet of the Pelletron facility to utilize the maximum proton current from the accelerator. The proton energy spread at the 6 m above the analyzing magnet of the Pelletron facility was 50–90 keV. At this port, the terminal voltage is regulated by generating voltage mode (GVM) by using a terminal potential stabilizer. Further, we used a collimator of 6-mm diameter before the target. The Li-metal foil with a thickness of 3.7 mg/cm² was sandwiched between two tantalum foils of different thicknesses. The front tantalum foil facing the proton beam was the thinnest one, with a thickness of 3.9 mg/cm², in which degradation of proton energy was only 30 keV [34]. On the other hand, the back tantalum foil was of 0.025 mm thick, which was sufficient to stop the proton beam. About 0.0657 gm (for 3.12 MeV) and 0.0166 gm (for 4.12 MeV) of manganese oxide (MnO_2) powder and 1-mm-thick natural indium metal foils of same size were wrapped separately with 0.025-mm-thick super pure aluminum foil. The size of the Al-wrapped MnO_2 powder sample was 1.0 cm² with a thickness of 29.3 mg/cm². The aluminum wrapper was used to stop and collect the reaction products recoiling out from the surface. Two different sets of Al-wrapped MnO_2 powder and In-metal stacks were prepared for different irradiations at the neutron energies of 3.12 and 4.12 MeV, respectively. The individual stacks of Al-wrapped MnO_2 powder and In-metal samples were additionally wrapped with two different Al foils. The sample was mounted at an angle of 0° with respect to the beam direction at a distance 2.1 cm behind the Ta–Li–Ta stack as described in Ref. [33]. The Ta–Li–Ta stack was bombarded with the proton energies (E_p) of 5 and 6 MeV for 13 h 25 min and 11 h 50 min, respectively. The proton current during the irradiations varied from 60 to 70 nA. Thus the Al-wrapped MnO_2 powder and In-metal stack faced the neutron energies (E_n) of 3.12 and 4.12 MeV for a period of 13 h 25 min and 11 h 50 min, respectively. After irradiation, the samples were cooled for 2 h 30 min and

2 h 9 min, respectively. Then, the irradiated target of Al wrapped manganese oxide powder and In-metal foils were mounted on different Perspex plate and taken for γ -ray spectrometry.

The experiments with the neutron energies of 1.12 and 2.12 MeV were performed by using the folded tandem ion beam accelerator (FOTIA) at Van-de-Graff, BARC, Mumbai. The neutron beam energies of 1.12 and 2.12 MeV were also produced from the $^7\text{Li}(p,n)^7\text{Be}$ reaction by using the proton beam energies of 3 and 4 MeV. In the present case, instead of Li-metal foil, a circular LiF pellet of 1 cm diameter and 3 mm thickness was used for neutron production. It was fixed on a stand at an angle 0° relative to the beam's exit window. A beam collimator of 10 mm diameter was used before the target. The 3 mm thick LiF pellet is sufficient to stop the proton beam energy of 3 and 4 MeV. About 0.0735 gm (for 1.12 MeV) and 0.0973 gm (for 2.12 MeV) of manganese sulfate ($(\text{MnSO}_4)\cdot 2\text{H}_2\text{O}$) powder and 1-mm-thick natural indium metal foils of same size were wrapped separately with 0.025-mm-thick super pure aluminum foil. The Al wrapped $(\text{MnSO}_4)\cdot 2\text{H}_2\text{O}$ powder and In-metal stacks were square shape having the size of 1.0 cm². The samples were mounted one at a time at 0° with respect to the beam direction at a distance of 3 mm behind the LiF pellet and irradiated for 8 h 32 min with neutron energy of 1.12 MeV and for 7 h 45 min with 2.12 MeV, respectively. For the proton energies of 3 and 4 MeV, the incident beam current during the irradiations was 100 nA. The irradiated samples were cooled for 1–2 h, mounted on different Perspex plates and taken for γ -ray spectrometry [33].

The γ -rays of the reaction products from the irradiated Mn and In samples were counted in an energy- and efficiency-calibrated, 80-cm³ high-purity germanium detector coupled to a personal computer-based 4K channel analyzer. The counting dead time was kept always <5% by placing the irradiated samples at a suitable distance from the detector to avoid pile up effects. The energy and efficiency calibration of the detector system was done by counting the γ -ray energies of a standard ^{152}Eu source by keeping the same geometry, where the summation error was negligible. This was checked by comparing the efficiency obtained from γ -ray counting of standards such as ^{241}Am (59.5 keV), ^{133}Ba (80.9, 276.4, 302.9, 356.0, and 383.8 keV), ^{137}Cs (661.7 keV), ^{54}Mn (834.6 keV), and ^{60}Co (1173 and 1332.5 keV). The detector efficiency was 20% at γ -ray energy of 1332.5 keV relative to the 73.5-mm-diameter and 73.5-mm-long NaI(Tl) detector. The uncertainty in the efficiency was 2–3%. The resolution of the detector system had a full-width at half-maximum of 1.8 keV at 1332.5 keV γ -ray energy of ^{60}Co . The γ -ray counting of the irradiated

Mn and In samples were done at least for three half-lives of the nuclides of interest.

3 Calculations

3.1 Calculation of neutron energy

In the present experiment, the fast neutrons were produced from the $^7\text{Li}(p,n)^7\text{Be}$ reaction by using the proton beam energies of 3, 4, 5 and 6 MeV. The Q -value for the $^7\text{Li}(p,n)^7\text{Be}$ reaction to the ground state is -1.644 MeV, whereas the first excited state is 0.431 MeV above the ground state leading to an average Q -value of -1.868 MeV. The threshold value of the $^7\text{Li}(p,n)$ reaction to the ground state of ^7Be is 1.881 MeV. Thus for the proton energies of 3, 4, 5 and 6 MeV, the resulting peak energy of the first group of neutrons (n_0) would be 1.12, 2.12, 3.12 and 4.12 MeV, respectively. The corresponding neutron energies of the second group of neutrons (n_1), for the first excited state of ^7Be , will be 0.63, 1.63, 2.63 and 3.63 MeV, respectively [35–37]. This is because above the proton energy of 2.37 MeV, the n_1 group of neutrons is also produced. Liskien and Paulsen [35] as well as Meadows and Smith [36] have given the branching ratio to the ground state and first excited state of ^7Be up to proton energy of 7 MeV. However, Poppe et al. [37] have given the branching ratio to the ground state and first excited state of ^7Be for proton energies from 4.2 to 26 MeV. Based on their [35–37] prescription for the proton energy of 6 MeV, the contribution to the n_0 and n_1 group of neutrons is $\sim 85\%$ and $\sim 15\%$, respectively. The proton energy of 6 MeV leads to an average neutron energy of $4.12 \times 0.85 + 3.63 \times 0.15 = 4.05$ MeV, which is within the uncertainty of neutron energy of 4.12. Thus the n_1 group neutrons have some contribution,

which causes the broadening of the main peak. This causes more uncertainty for the emitted neutrons energies under the main peak. Thus for the proton energies of 3, 4, 5 and 6 MeV, the energies of the emitted neutrons were estimated to be 1.12 ± 0.11 , 2.12 ± 0.15 , 3.12 ± 0.21 , and 4.12 ± 0.32 MeV, respectively. Above the proton energy of 4.5 MeV, the neutron spectrum consists of the full energy peak due to the $^7\text{Li}(p,n)^7\text{Be}$ reaction and a continuum component attributable to the multi-body break up process, i. e. $^7\text{Li}(p,n^3\text{He})^4\text{He}$ reaction with Q value of -3.231 MeV. This causes a continuous neutron energy distribution as tail besides n_0 and n_1 groups of neutrons. Up to the proton energy of 5 MeV, there is no tail part in the neutron spectrum [33]. For the proton energy of 6 MeV, there is very small tail part [33], which can be neglected in the calculation of average neutron energy and thus in the $^{55}\text{Mn}(n,\gamma)^{56}\text{Mn}$ reaction cross-section.

3.2 Calculation of neutron flux and $^{55}\text{Mn}(n,\gamma)^{56}\text{Mn}$ reaction cross-section

In the present work, the $^{115}\text{In}(n,\gamma)^{116\text{m}}\text{In}$ reaction cross-section was used as the neutron flux monitor. The photo-peak activities of the 138.3, 416.9, 818.7, 1097.3 and 1293.6 keV γ -lines of $^{116\text{m}}\text{In}$ from the $^{115}\text{In}(n,\gamma)$ reaction were used for the neutron flux determination. On the other hand, the photo-peak activity of the 846.8 keV γ -ray of ^{56}Mn was used for the calculation of $^{55}\text{Mn}(n,\gamma)$ reaction cross-section. The nuclear spectroscopic data used in the calculation were taken from Ref. [38] and shown in the Table 1. The numbers of detected γ -rays (A_{obs}) for the reaction products $^{116\text{m}}\text{In}$ and ^{56}Mn were obtained from the total peak areas after subtracting the linear Compton background.

It can be seen from Table 1 that the reaction product $^{116\text{m}}\text{In}$ has a half-life of 54.29 min with five significant

Table 1: Nuclear spectroscopic data of the radio-nuclides from the $^{115}\text{In}(n,\gamma)^{116\text{m}}\text{In}$ and $^{55}\text{Mn}(n,\gamma)^{56}\text{Mn}$ reactions used in the calculation from Ref. [38].

Nuclide	Spin-Parity	Half-life	Decay mode (%)	γ -ray energy (keV)	γ -ray abundance (%)
$^{116\text{m}}_{49}\text{In}$	8^-	2.18 ± 0.04 s	IT (100%)	–	–
$^{116\text{m}}_{49}\text{In}$	5^+	54.29 ± 0.17 min	β^- (100%)	138.3	3.70 ± 0.09
				416.9	27.2 ± 0.4
				818.7	12.13 ± 0.14
				1097.3	58.5 ± 0.8
				1293.6	84.8 ± 0.12
$^{116\text{g}}_{49}\text{In}$	1^+	14.10 ± 0.03 s	β^- (99.98%) and ε (0.02%)	463.3	0.25
				1293.4	1.3
$^{56}_{25}\text{Mn}$	3^+	2.5789 ± 0.0001 h	β^- (100%)	846.8	98.85

The γ -line marked with bold letters were adopted for data reduction.

γ -lines with good branching intensities. From the photo-peak activity (A_{obs}) of the 138.3, 416.9, 818.7, 1097.3 and 1293.6 keV γ -lines of $^{116\text{m}}\text{In}$, the neutron flux (Φ) was obtained by using the following equation [33].

$$\Phi = \frac{A_{\text{obs}} \left[\frac{CL}{LT} \right] \lambda}{N \sigma_R I_\gamma \varepsilon (1 - e^{-\lambda t}) (e^{-\lambda T}) (1 - e^{-\lambda CL})} \quad (1)$$

where, N is the number of target atoms and σ_R is the cross-section of the $^{115}\text{In}(n,\gamma)^{116\text{m}}\text{In}$ reaction. λ is the decay constant ($\lambda = \ln 2 / T_{1/2}$) of the reaction product of interest with half-life = $T_{1/2}$. I_γ is the branching intensity of the 138.33, 416.86, 818.72, 1097.33 and 1293.56 keV γ -lines of $^{116\text{m}}\text{In}$ [38] and ε is its detection efficiency. t , T , CL and LT are the irradiation time, cooling time, real and live-time of counting, respectively.

The $^{115}\text{In}(n,\gamma)^{116\text{m}}\text{In}$ reaction cross-section is available for a wide range of neutron energies in the literature, which is compiled in EXFOR [12]. However, the $^{115}\text{In}(n,\gamma)^{116\text{m}}\text{In}$ reaction cross-sections within the neutron energy range of 1.96–7.66 MeV are available in the Refs. [30, 39–41]. Among them, the cross-sections obtained by Husain et al. [40] are within the neutron energy range of 2.44–4.5 MeV and are higher than the data of others [30, 39, 41]. Thus the $^{115}\text{In}(n,\gamma)^{116\text{m}}\text{In}$ reaction cross-sections from the Refs. [30, 39, 41] were used in the present work for the neutron flux calculation. The evaluated $^{115}\text{In}(n,\gamma)^{116\text{m}}\text{In}$ reaction cross-sections as a function of neutron energy are available in the IRDFF-1.05 library [42]. Thus the neutron flux based on the evaluated $^{115}\text{In}(n,\gamma)^{116\text{m}}\text{In}$ reaction cross-sections were also used to determine the neutron flux. The $^{115}\text{In}(n,\gamma)^{116\text{m}}\text{In}$ reaction cross-section from Refs. [30, 39, 41, 42] and neutron flux obtained for the four neutron energies of present work are given in the Table 2.

From the photo-peak activity of 846.8 keV γ -ray of ^{56}Mn , the $^{55}\text{Mn}(n,\gamma)$ reaction cross-section (σ_R) was calculated by using the rearranged equation (1). The nuclear

spectroscopic data used were taken from Table 1 based on the Ref. [38]. The neutron flux (Φ) from Table 2 was used to calculate the $^{55}\text{Mn}(n,\gamma)^{56}\text{Mn}$ reaction cross-section. The neutron self shielding effect of the sample and its correction factor is important in the calculations of $^{55}\text{Mn}(n,\gamma)^{56}\text{Mn}$ reaction cross-section. In particular, the neutron self shielding is very much important in the resonance cross-section region and for the big size of sample [43, 44]. The neutron self shielding factor is the ratio of the mean fluence rate inside the sample volume to the fluence rate incident on the sample [44]. A complete treatment of self-shielding requires consideration of the neutron energy spectrum inside and outside the sample, the absorption and scattering cross sections as well as the size of the sample [44]. In the present case, the sizes of the sample and reaction monitor are very small. The $^{55}\text{Mn}(n,\gamma)^{56}\text{Mn}$ and the $^{115}\text{In}(n,\gamma)^{116\text{m}}\text{In}$ reactions cross-sections in the neutron energies of present work are not in the resonance region. The scattered neutrons from the surrounding were not available due to the absence of neutron shielding wall far from the experimental set up. Besides this, the $^{115}\text{In}(n,\gamma)^{116\text{m}}\text{In}$ and $^{55}\text{Mn}(n,\gamma)^{56}\text{Mn}$ reaction cross-sections as a function of neutron energy have similar patterns. If any low energy scattered neutrons will be there from far surrounding wall then also their effect will get canceled due to the similar trend of reaction cross-sections of the sample and monitor. Thus the neutron self shielding effect for the sample size of present work will be negligible and was not considered in the calculation of $^{55}\text{Mn}(n,\gamma)^{56}\text{Mn}$ reaction cross-section.

4 Results and discussion

The $^{55}\text{Mn}(n,\gamma)^{56}\text{Mn}$ reaction cross-section determined in the present work for the neutron energies of 1.12, 2.12, 3.12 and 4.12 MeV were given in the Table 2. The overall

Table 2: $^{115}\text{In}(n,\gamma)^{116\text{m}}\text{In}$ and $^{55}\text{Mn}(n,\gamma)^{56}\text{Mn}$ reaction cross-sections at different neutron energies.

Proton energy (MeV)	En (MeV)	$^{115}\text{In}(n,\gamma)^{116\text{m}}\text{In}$ reaction cross section (mb) [Ref.]	Flux n/cm ² s	$^{55}\text{Mn}(n,\gamma)^{56}\text{Mn}$ reaction cross section	
				Experimental (mb)	TALYS-1.6 (mb)
3	1.12 ± 0.12	247.1 ± 28.6 [30]	5.67099E+06	3.374 ± 0.487	3.872
		174.4 ± 6.7 [42]	8.03273E+06	2.382 ± 0.344	
4	2.12 ± 0.15	129.0 ± 9.1 [39]	1.29330E+07	2.563 ± 0.147	3.031
		104.1 ± 4.5 [42]	1.51154E+07	2.062 ± 0.126	
5	3.12 ± 0.21	44.6 ± 3.2 [41]	2.03785E+07	1.407 ± 0.136	1.721
		37.5 ± 1.5 [42]	2.41184E+07	1.184 ± 0.117	
6	4.12 ± 0.32	16.7 ± 2.4 [41]	7.23707E+07	1.137 ± 0.178	1.149
		15.7 ± 0.7 [42]	7.72136E+07	1.066 ± 0.167	

uncertainty associated with the measured $^{55}\text{Mn}(n,\gamma)^{56}\text{Mn}$ reaction cross-section is the quadratic sum of both statistical and systematic errors. The random error in the observed γ -ray activity of ^{56}Mn is primarily due to counting statistics, which is estimated to be 3.1–5.5%. This can be determined by accumulating the data for an optimum time period that depends on the half-life of the nuclide of interest. The systematic errors are due to uncertainties in the irradiation time ($\sim 0.1\%$), the half-life of the reaction products and the γ -ray abundances (1–2%) and the detection efficiency ($\sim 3\%$), which arises from the fitting error. The maximum systematic error (3.8–14.4%) is primarily due to the uncertainty in the $^{115}\text{In}(n,g)^{116\text{m}}\text{In}$ reaction cross-section [30, 39–42], which reflect in the neutron flux and thus in the $^{55}\text{Mn}(n,\gamma)^{56}\text{Mn}$ reaction cross-section. Thus the total systematic error is 4.9–14.8%. The combined uncertainties from both statistical and systematic errors lie within 5.8–15.8% for the $^{55}\text{Mn}(n,\gamma)^{56}\text{Mn}$ reaction cross-section.

The $^{55}\text{Mn}(n,\gamma)^{56}\text{Mn}$ reaction cross-section at the neutron energies of 4.12 MeV is determined in the present work for the first time. Sufficient data are available in literature [13–30] within the neutron energy of 4 MeV and within 13.4–15.7 MeV. Besides this, one set of data within the neutron energies of 0.97–19.4 MeV is available in Ref. [19]. In view of this, the present data and literature data [16–30] within neutron energy of 0.5–19.4 MeV are plotted in Figure 1. It can be seen from Figure 1 that the literature data [16, 17, 19, 21, 29, 30] within neutron energies of 0.5–3.43 MeV follows three different trends. The data of Gautam et al. [30] is on higher side. The data of Stavisskiy et al.

[17], Menlove et al. [19] and Dovbenko et al. [21] within the neutron energy of 3.43 MeV are on the lower side. On the other hand, the data of Johnsurd et al. [16] and Trofimov et al. [29] within the neutron energy of 3.43 MeV are in between those two above sets. The experimental data of present work at the neutron energies of 1.12 and 2.12 MeV are in between the data of two sets but are in close agreement with the data of Johnsurd et al. [16] and Trofimov et al. [29]. At the neutron energy of 3.12 MeV, the present data is in agreement with the data of Menlove et al. [19] and Dovbenko et al. [21]. Similarly, the present data at the neutron energy of 4.12 MeV is in agreement with the data of Menlove et al. [19]. It can be also seen from Figure 1 that within neutron energy of 3.43 MeV, there is a lot of differences in the three sets of literature data [16, 17, 19, 21, 29]. In view of this the $^{55}\text{Mn}(n,\gamma)^{56}\text{Mn}$ reaction cross-section within neutron energies of 1–20 MeV was calculated theoretically by using the computer code TALYS 1.6 [31] and EMPIRE 3.2.2 [32].

TALYS is a computer code for the prediction and analysis of nuclear reactions. TALYS has two main purposes; it can be used as a nuclear physics tool, confronting nuclear models with experiments and secondly, as a nuclear data tool, predicting nuclear data where no experimental data exists. The TALYS-1.6 program [31] simulates nuclear reactions that involve gammas, neutrons, protons, deuterons, tritons, ^3He and alpha-particles in the incident energy range from 1 keV to 200 MeV for target nuclides of mass 12 and heavier. In the present work, we have used neutron energies from 1 keV to 20 MeV for the ^{55}Mn target. All possible outgoing channels including inelastic were considered for a given projectile (neutron) energy. However, the cross-sections for the (n,γ) reactions were specially looked for and collected. Theoretically calculated $^{55}\text{Mn}(n,\gamma)^{56}\text{Mn}$ reaction cross-sections from a neutron energy of 1 to 20 MeV using TALYS version 1.6 are also plotted in Figure 1.

EMPIRE-3.2.2 [32] is a modular system of nuclear reaction codes, implementing the major reaction mechanisms, such as compound nucleus (in the Hauser–Feshbach model with width fluctuation correction [45]), pre-equilibrium emission (by means of the exciton model or the hybrid Monte Carlo simulation approach) and direct interaction (using various optical model parameters automatically retrieved from the Reference Input Parameter Library (RIPL-2) library [46] or chosen by the user). It includes various nuclear models, designed for calculations in a broad range of energies and incident particles. In the present work, EMPIRE-3.2.2 [32] was used with the default parameters for nuclear masses, ground-state deformations, discrete levels, decay schemes, level

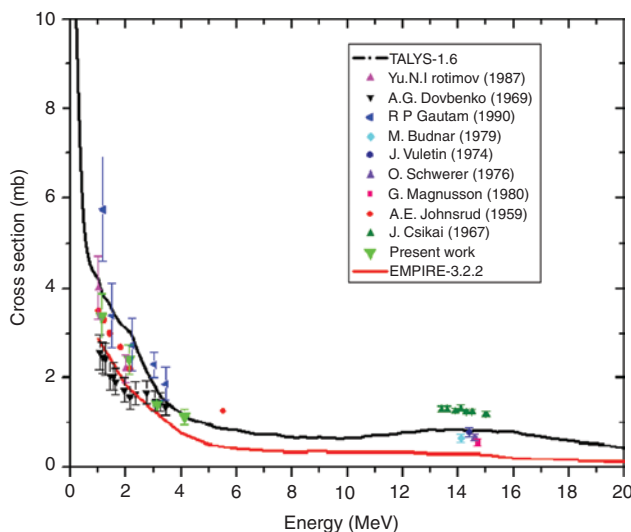


Figure 1: Comparison of experimental $^{55}\text{Mn}(n,\gamma)^{56}\text{Mn}$ reaction cross-section from the present work and literature data [13–30] with the theoretical values from TALYS 1.6 [31] and EMPIRE-3.2.2 [32].

densities, moments of inertia (MOMFIT) and strength functions. Theoretically calculated $^{55}\text{Mn}(n,\gamma)^{56}\text{Mn}$ reaction cross-sections from a neutron energy of 1–20 MeV using EMPIRE-3.2.2 [32] are also plotted in Figure 1.

It can be seen from Figure 1 that the experimental data of Gautam et al. [30] and some data of Trofimov et al. [29] is in closer to the theoretical values of TALYS 1.6 [31], whereas data of Stavisskiy et al. [17], Menlove et al. [19] and Dovbenko et al. [21] within 3.43 MeV are closer to the theoretical values of EMPIRE-3.2.2 [32]. On the other hand, the present data as well as the literature data of Johnsrud et al. [16] within 3.43 MeV are in between the theoretical values of TALYS 1.6 [31] and EMPIRE-3.2.2 [32]. Similarly, the data from the literature [14, 22–27] around 14 MeV are in between the theoretical values of TALYS 1.6 [31] and EMPIRE-3.2.2 [32]. On the other hand, the data of Johnsrud et al. [16] at the neutron energy of 5.5 MeV and Csikai et al. [18] around 13.4–15 MeV are higher than the theoretical values of TALYS 1.6 [31] and EMPIRE-3.2.2 [32]. The present data at the neutron energy of 4.12 MeV and the data of Menlove et al. [19] from 4 to 19.39 MeV are in close agreement with the theoretical values of TALYS 1.6 [31].

5 Conclusions

The $^{55}\text{Mn}(n,\gamma)^{56}\text{Mn}$ reaction cross-section at the neutron energies of 1.12, 2.12, 3.12 and 4.12 MeV are determined by using activation and off-line gamma ray spectrometric technique. They are found to in agreement with one set of experimental data from literature but not with the other two sets of literature data. The $^{55}\text{Mn}(n,\gamma)^{56}\text{Mn}$ reaction cross-section also calculated theoretical values of TALYS 1.6 and EMPIRE-3.2.2. The present data for the neutron energies of 1.12, 2.12 and 3.12 MeV are found to be in between the theoretical values of TALYS 1.6 and EMPIRE-3.2.2. On the other hand present data at the neutron energy of 4.12 MeV is in agreement with the theoretical values of TALYS 1.6.

Acknowledgments: One of the authors, Vibha Vansola, is thankful to Dr. J. P. Singh, Head, Department of Physics, M. S. University, Baroda and UGC-BSR for encouraging us to carry out this work and for their valuable suggestions and for the fellowship. The authors also thankful to the staff of the FOTIA at Van-de-Graff, BARC and Pelletron facility, TIFR for their excellent operation of the accelerator and giving the proton beam during the irradiation.

References

1. Sinha, R. K., Kakodkar, A.: Design and development of the AHWR – the Indian thorium fuelled innovative nuclear reactor. *Nucl. Eng. Des.* **236**, 683 (2006).
2. Allen, T. R., Crawford, D. C.: Lead-cooled fast reactor systems and the fuels and materials challenges. *Sci. Technol. Nucl. Install.*, **2007**, 11 (2007).
3. Nuttin, A., Heuer, D., Billebaud, A., Brissot, R., Le Brun, C., Liatard, E., Loiseaux, J. M., Mathieu, L., Meplan, O., Merle-Lucotte, E., Nifenecker, H., Perdu, F., David, S.: Potential of thorium molten salt reactors detailed calculations and concept evolution with a view to large scale energy production. *Prog. Nucl. Energy* **46**, 77 (2005).
4. Mathieu, L., Heuer, D., Brissot, R., Garzenne, C., Lebrun, C., Liatard, E., Loiseaux, J. M., Meplan, O., Merle-Lucotte, E., Nuttin, A.: Proportion for a very simple thorium molten salt reactor, in Proceedings of the Global International Conference, Paper No. 428, Tsukuba, Japan, 2005.
5. Fast reactors and accelerator driven systems knowledge base, IAEA-TECDOC-1319: thorium fuel utilization: options and trends (Nov. 2002).
6. Carminati, F., Klapisch, R., Revol, J. P., Roche, Ch., Rubia, J. A., Rubia, C.: An energy amplifier for cleaner and inexhaustible nuclear energy production driven by particle beam accelerator. *CERN/AT/93-49 (ET)* 1993.
7. Arthur, E. D., Schriber, S. A., Rodriguez, A. (Editors): The international conference on accelerator-driven transmutation technologies and applications. Las Vegas, Nevada, USA, 1994, AIP Conf. Proc., Vol. 346 (1995).
8. Rubia, C., Rubio, J. A., Buono, S., Carminati, F., Fietier, N., Galvez, J., Geles, C., Kadi, Y., Klapisch, R., Mandrillon, P., Revol, J. P., Roche, Ch.: Conceptual design of a fast neutron operated high power energy amplifier. *CERN/AT/95-44 (ET)* 1995.
9. Accelerator driven systems: energy generation and transmutation of nuclear waste. status report, IAEA, Vienna, IAEA-TECDOC-985, 1997.
10. Bowman, C. D.: Accelerator driven systems for nuclear waste transmutation. *Ann. Rev. Nucl. Part. Sci.* **48**, 505 (1998).
11. Kapoor, S. S.: Accelerator-driven sub-critical reactor system (ADS) for nuclear energy generation. *Pramana-J. Phys.* **59**, 941 (2002).
12. Otuka, N., Dupont, E., Semkova, V., Pritychenko, B., Blokhin, A. I., Aikawa, M., Babykina, S., Bossant, M., Chen, G., Dunaeva, S., Forrest, R. A., Fukahori, T., Furutachi, N., Ganesan, S., Ge, Z., Gritzay, O. O., Herman, M., Hlavač, S., Kato, K., Lalremruata, B., Lee, Y. O., Makinaga, A., Matsumoto, K., Mikhaylyukova, M., Pikulina, G., Pronyaev, V. G., Saxena, A., Schwerer, O., Simakov, S. P., Soppera, N., Suzuki, R., Takács, S., Tao, X., Taova, S., Tárkányi, F., Varlamov, V. V., Wang, J., Yang, S. C., Zerkov, V., Zhuang, Y.: Experimental nuclear reaction data. *Nucl. Data Sheets* **120**, 272 (2014).
13. Leipunskiy, A. I., Kazachkovskiy, O. D., Artyukhov, G. J., Baryshnikov, A. I., Belanova, T. S., Galkov, V. I., Stavisskiy, Y. J., Stumbur, E. A., Sherman, L. E.: Radiative capture cross-section measurements for fast neutrons. *Fiziko-Energeticheskii Inst., Obninsk, Russia, second UN Conf. on the Peaceful Uses of Atomic Energy. Geneva, 1–13 Sep 1958, 15, 50(2219) 1958.*

14. Perkin, L., O'Connor, L. P., Coleman, R. F.: Radiative capture cross sections for 14.5 MeV neutrons. *Proc. Physical Soc.* **72**, 505 (1958).
15. Bostrom, N. A., Morgan I. L., Prud'homme, J. T., Okhuysen, P. L., Hundson Jr, O. M.: Neutron interactions in lithium, carbon, nitrogen, aluminium, argon, manganese, yttrium, zirconium, radiolead and bismuth. Report No. WADC-TN-59-107, 1959.
16. Johnsrud, A. E., Silbert, M. G., Barschall, H. H.: Energy dependence of fast-neutron activation cross section. *Phys. Rev.* **116**, 927 (1959).
17. Stavisskiy, J. Y., Tolstikov, V. A.: Radiative neutron cross-section for several isotopes in the energy range 0.03–2.5 MeV. *Atomnaya Energiya* **10**(5), 508 (1961).
18. Csikai, J., Peto, G., Buczko, M., Milligy, Z., Eissa, N.: Radiative capture cross-sections for 14.7 MeV neutrons. *Nucl. Phys. A* **95**, 229 (1967).
19. Menlove, H. O., Coop, K. L., Grench, H. A., Sher, R.: Neutron radiative capture cross sections for Na23, Mn55, In115, and Ho165 in the energy range 1.0 to 19.4 MeV. *Phys. Rev.* **163**, 1299 (1967).
20. Peto, G., Milligy, Z., Hunyadi, I.: Radiative capture cross-sections for 3 MeV neutrons. *J. Nucl. Energy.* **21**, 797 (1967).
21. Dovbenko, A. G., Kolesov, V. E., Koroleva, V. P., Tolstikov, V. A.: A determination of the 2200 M/S absorption cross section and resonance integral of arsenic by pile oscillator technique. *Soviet Atomic Energy* **26**, 82 (1969).
22. Vuletin, J., Kulisic, P., Cindro, N.: Activation cross-sections of (n, gamma) reactions at 14 MeV. *Lettere al Nuovo Cimento* **10**, 1 (1974).
23. Schwerer, O., Winklerrohatsch, M., Warhanek, H., Winkler, G.: Measurement of cross-sections for 14 MeV neutron capture. *Nucl. Phys. A* **264**, 105 (1976).
24. Manjushree, Majumder, B. Mitra, B.: Capture cross section of 14 MeV neutrons. *Trans. Bose Research Inst., Calcutta* **40**(3), 81 (1977).
25. Budnar, M., Cvelbar, F., Hodgson, E., Hudoklin, A., Ivkovic, V., Likar, A., Mihailovic, M. V., Martincic, R., Najzer, M., Perdan, A., Potokar, M., Ramsak, V.: Prompt gamma-ray spectra and integrated cross sections for the radiative capture of 14 MeV neutrons for 28 natural targets in the mass region from 12 to 208. *INDC (YUG)-6*, 1979.
26. Magnusson, G., Andersson, P., Berquist, I.: 14.7 MeV neutron capture cross-section Measurements. *Physica Scripta* **21**(1), 21 (1980).
27. Bahal, B. M., Pepelnik, R.: Cross section measurements of Cr, Mn, Fe, Co, Ni for an accurate determination of these elements in natural and synthetic samples using a 14 MeV neutron generator. *Ges. Kernenergie, Schiffbau und Schifffahrt* **E**(85), 11 (1985).
28. Trofimov, Y. N.: Neutron radiation capture cross-sections for nuclei of medium and large masses at the neutron energy 1 MeV. *Int. Conf. on Neutron Physics, Kiev, 14–18 Sep 1987, Vol. 3*, p. 331 (1987).
29. Trofimov, Y. N.: Activation cross-sections for 31 nuclei at the neutron energy 2 MeV. *Vop. At. Nauki i Tekhn., Ser. Yadernye Konstanty*, **1987**(4), 10 (1987).
30. Gautam, R. P., Singh, R. K., Rizvi, I. A., Afzal Ansari, M., Chaubey, A. K., Kailas, S.: Measurement of radiative capture of fast neutrons in Mn-55 and In-115. *Indian J. Pure Appl. Phys.* **28**, 235 (1990).
31. Koning, A. J., Hilaire, S., Duijvestijn, M. C.: TALYS-1.6, A nuclear reaction Program. NRG-1755 NG Petten, The Netherlands, 2008, <http://www.talys.eu>.
32. Herman, M.: Empire-II statistical model code for nuclear reaction calculations. IAEA, Vienna (2002).
33. Vansola, V., Ghosh, R., Badwar, S., Lawriniang, B. M., Gopalakrishna, A., Naik, H., Naik, Y., Tawade, N. S., Sharma, S. C., Bhatt, J. P., Gupta, S. K., Sarode, S., Mukherjee, S., Singh, N. L., Singh, P., Goswami A.: Measurement of $^{197}\text{Au}(n,\gamma)^{198}\text{Au}$ reaction cross-section at the neutron energies of 1.12, 2.12, 3.12 and 4.12 MeV. *Radiochim. Acta* **103**, 817 (2015).
34. Ziegler, J. F.: SRIM-2003. *Nucl. Instru. Methods Phys. Res. B* **219–220**, 1027 (2004). Available at <http://www.srim.org/>.
35. Liskien, H., Paulsen, A.: Neutron production cross-sections and energies for the reactions $^7\text{Li}(p,n)^7\text{Be}$ and $^7\text{Li}(p,n)^7\text{Be}^*$. *At. Data Nucl. Data Tables* **15**, 57 (1975).
36. Meadows, J. W., Smith, D. L.: Neutrons from proton bombardment of natural Lithium. Argonne National Laboratory Report ANL-7983 (1972).
37. Poppe, C. H., Anderson, J. D., Davis, J. C., Grimes, S. M., Wong, C.: Cross sections for the $^7\text{Li}(p,n)^7\text{Be}$ reaction between 4.2 and 26 MeV. *Phys. Rev. C* **14**, 438 (1976).
38. NuDat 2.6, National Nuclear Data Center, Brookhaven National Laboratory. Available at: <http://www.nndc.bnl.gov/> (2011).
39. Andersson, P., Zorro, R., Bergqvist, I.: On neutron capture cross-section measurements with the activation technique in the MeV region. *Conf. on Nucl. Data for Sci. And Technol*, K.H. Bockhoff (editor), Antwerp, Belgium, Sept. 6–10, Page 866, 1982, published by D. Reidel Publishing Company, P. O. Box 17, 3300 AA Dordrecht, Holland.
40. Husain, H. A., Hunt, S. E.: Absolute neutron cross section measurements in the energy range between 2 and 5 MeV. *Int. J. Appl. Radiat. Isot.* **34**, 731 (1983).
41. Andersson, P., Zorro, R., Berqvist, I., Herman, M., Marcinkowski, A.: Cross Sections for $^{197}\text{Au}(n,\gamma)^{198}\text{Au}$ and $^{115}\text{In}(n,\gamma)^{116}\text{mIn}$ in the Neutron Energy Region 2.0–7.7 MeV. *Nucl. Phys. A* **443**, 404 (1985).
42. Zolotarev, K. I., Zolotarev, P. K.: Evaluation of the excitation functions for the $^{54}\text{Fe}(n, p)^{54}\text{Mn}$, $^{58}\text{Ni}(n, 2n)^{57}\text{Ni}$, $^{67}\text{Zn}(n, p)^{67}\text{Cu}$, $^{92}\text{Mo}(n, p)^{92\text{m}}\text{Nb}$, $^{93}\text{Nb}(n,\gamma)^{94}\text{Nb}$, $^{113}\text{In}(n, n')^{113\text{m}}\text{In}$, $^{115}\text{In}(n,\gamma)^{116\text{m}}\text{In}$, and $^{169}\text{Tm}(n, 3n)^{167}\text{Tm}$ reactions. Progress Report on Research Contract No 16242, INDC (NDS)-0657. Available at <https://www-nds.iaea.org/publications/indc/indc-nds-0657.pdf> (2013).
43. Lindstrom, R. M., Ronald F., Fleming, R. F.: Neutron self-shielding factors for simple geometries, revisited. *Chem. Anal. (Warsaw)* **53**, 855 (2008).
44. Trkov, A., Zerovnik, G., Snoj, L., Ravnik, M.: On the self-shielding factors in neutron activation analysis. *Nucl. Instru. Meth. Phys. Res. A* **610**, 553 (2009).
45. Hofmann, H., Richert, J., Tepel, J., Weidenmuller, H.: Cross sections for the $^7\text{Li}(p,n)^7\text{Be}$ reaction between 4.2 and 26 MeV. *Ann. Phys.* **90**, 403 (1975).
46. Belgya, T., Bersillon, O., Capote, R., Fukahori, T., Zhigang, G., Goriely, S., Herman, M., Ignatyuk, A. V., Kailas, S., Koning, A., Oblozinsky, P., Plujko, V., Young, P.: RIPL-2 Reference input parameter library, RIPL-2. IAEA- TECDOC-1506, Vienna. Available at: <http://www-nds.iaea.org/ripl2/> (2006).